Draft version July 7, 2011
Preprint typeset using LaTeX style emulateapj v. 11/10/09



# 1 $\mu$M EXCESS SOURCES IN THE UKIDSS. I. THREE T DWARFS IN THE SLOAN DITITAL SKY SURVEY SOUTHERN EQUATORIAL STRIPE

Y. Matsuoka[1], B. A. Peterson[2], K. L. Murata[1], M. Fujiwara[1], T. Nagayama[1], T. Suenaga[3], K. Furusawa[4], N. Miyake[4], K. Omori[4], D. Suzuki[5], and K. Wada[5]

*Draft version July 7, 2011*

## ABSTRACT

We report the discovery of two field brown dwarfs, ULAS J0128−0041 and ULAS J0321+0051, and the rediscovery of ULAS J0226+0051 (IfA 0230-Z1), in the Sloan Digital Sky Survey (SDSS) southern equatorial stripe. They are found in the course of our follow-up observation program of 1-$\mu$m excess sources in the United Kingdom Infrared Telescope Infrared Deep Sky Survey. The Gemini Multi-Object Spectrographs spectra at red optical wavelengths (6500–10500 Å) are presented, which reveal that they are early-T dwarfs. The classification is also supported by their optical to near-infrared colors. It is noted that ULAS J0321+0051 is one of the faintest currently-known T dwarfs. The estimated distances to the three objects are 50–110 pc, thus they are among the most distant field T dwarfs known. Dense temporal coverage of the target fields achieved by the SDSS-II Supernova Survey allows us to perform a simple time-series analysis, which leads to the finding of significant proper motions of 150–290 mas yr$^{-1}$ or the transverse velocities of 40–100 km s$^{-1}$ for ULAS J0128−0041 and ULAS J0226+0051. We also find that there are no detectable, long-term (a-few-year) brightness variations above a few times 0.1 mag for the two brown dwarfs[a].

*Subject headings:* brown dwarfs — stars: individual (ULAS J0128−0041, ULAS J0226+0051, ULAS J0321+0051) — stars: low-mass — surveys

## 1. INTRODUCTION

Brown dwarfs are low-mass substellar objects which could not ignite hydrogen fusion in their collapsing phases. They occupy the transition zone between stars and planets in the physical parameters such as mass and temperature, hence their studies provide vital information on the formation of both populations. However, their dim nature has prevented the discovery of brown dwarfs despite the great efforts made by the early observers (see Kirkpatrick 2005, for a review). The presence of the population was first confirmed observationally by the discovery of GD 165B (Becklin & Zuckerman 1988) and Gl 229B (Nakajima et al. 1995), which are now classified as spectral types L and T, respectively.

Thanks to the advent of the wide-field surveys such as the Sloan Digital Sky Survey (SDSS; York et al. 2000), the Two Micron All Sky Survey (2MASS; Skrutskie et al. 2006), the Deep Near Infrared Survey of the Southern Sky (DENIS; Epchtein et al. 1999), the United Kingdom Infrared Telescope (UKIRT) Infrared Deep Sky Survey (UKIDSS; Lawrence et al. 2007), and the Canada-France Brown Dwarf Survey (Delorme et al. 2008), brown dwarfs are now continuously being found. About 600 L dwarfs and 200 T dwarfs are known today (compiled in the DwarfArchive.org[6]), and the focus of the latest surveys tends to be on the discovery of the latest T and even cooler Y dwarfs. On the other hand, the number of known early-T dwarfs is still small, only 10–20 objects in a spectral subclass.

Nonetheless, early-T dwarfs represent some key phenomena necessary for understanding the whole brown dwarf population. One such phenomenon is the so-called $J$-band brightening (Dahn et al. 2002; Knapp et al. 2004; Vrba et al. 2004), wherein early-T dwarfs have higher $J$-band luminosity than earlier type objects which should have hotter temperatures. It is interesting to note that a higher binary frequency of the L/T transition objects relative to early/mid-L and mid/late-T subclasses are suggested (Burgasser et al. 2005), which may be related to the cause of the $J$-band brightening (Liu et al. 2006). While it is actively attempted to construct the models of their atmospheres in order to parameterize their observational behaviors, the small number of known objects has hampered conclusive arguments about the statistical properties of the population.

In this paper we report the discovery of two field early-T dwarfs, as well as the rediscovery of one, in the SDSS southern equatorial stripe. The dense temporal coverage achieved by the SDSS-II Supernova Survey allows

[1] Graduate School of Science, Nagoya University, Furo-cho, Chikusa-ku, Nagoya 464-8602, Japan; matsuoka@a.phys.nagoya-u.ac.jp
[2] Mount Stromlo Observatory, Research School of Astronomy and Astrophysics, Australian National University, Weston Creek P.O., ACT 2611, Australia.
[3] Department of Astronomical Sciences, Graduate University for Advanced Studies (Sokendai), 2-21-1 Osawa, Mitaka, Tokyo 181-8588, Japan.
[4] Solar-Terrestrial Environment Laboratory, Nagoya University, Nagoya 464-8601, Japan.
[5] Department of Earth and Space Science, Osaka University, Osaka, 560-0043, Japan.
[a] Based on observations obtained at the Gemini Observatory, which is operated by the Association of Universities for Research in Astronomy, Inc., under a cooperative agreement with the NSF on behalf of the Gemini partnership: the National Science Foundation (United States), the Science and Technology Facilities Council (United Kingdom), the National Research Council (Canada), CONICYT (Chile), the Australian Research Council (Australia), Ministério da Ciência e Tecnologia (Brazil) and Ministerio de Ciencia, Tecnología e Innovación Productiva (Argentina).

[6] http://spider.ipac.caltech.edu/staff/davy/ARCHIVE/index.shtml

us to constrain their transverse velocities and variability. This is the first paper from our follow-up observation program of 1 $\mu$m excess sources in the UKIDSS. We give a minimum description of the observation strategy in the following section, while the full description is given in a companion paper (Y. Matsuoka et al. 2011, in preparation). Throughout this paper, magnitudes are given in the AB system for the SDSS optical bands and in the Vega system for the UKIDSS near-IR bands.

## 2. OBSERVATIONS

### 2.1. *Target Selection*

The three T dwarfs, ULAS J0128−0041 (R.A. $01^{\rm h}28^{\rm m}14^{\rm s}.41$, decl. $-00^\circ41^{\rm m}53^{\rm s}.5$), ULAS J0226+0051 (R.A. $02^{\rm h}26^{\rm m}37^{\rm s}.55$, decl. $+00^\circ51^{\rm m}54^{\rm s}.4$), and ULAS J0321+0051 (R.A. $03^{\rm h}21^{\rm m}22^{\rm s}.98$, decl. $+00^\circ51^{\rm m}05^{\rm s}.2$), are found on the UKIDSS Large Area Survey (LAS) images of the SDSS[7] southern equatorial stripe, also known as the stripe 82, where the SDSS-II Supernova Survey has been carried out (Frieman et al. 2008). The SDSS $i$, $z$ and the UKIDSS $Y$-, $J$-, $H$-, and $K$-band magnitudes of the targets are summarized in Table 1[8]. Note that the UKIDSS $2''.8$ aperture is larger enough than the typical seeing of $0''.8$ (Warren et al. 2007), so that the aperture losses have little influence on this work. The targets have been selected in the course of our follow-up observation program of 1 $\mu$m excess sources in the UKIDSS (Y. Matsuoka et al. 2011, in preparation). Their extremely red $i-Y$ ($i_{\rm AB}-Y_{\rm Vega}>5$) and blue $Y-J$ ($Y_{\rm Vega}-J_{\rm Vega}<1$) colors, along with the stellar appearances, suggested that they can be either of the two rare populations, i.e., highest-redshift ($z>6.5$) quasars or brown dwarfs (e.g., Venemans et al. 2007). The discovery of the former objects are our ultimate goal, which has not been achieved in the previous projects such as the SDSS quasar survey (Fan et al. 2006, and references therein), the Canada–France High-$z$ Quasar Survey (Willott et al. 2010, and references therein), and the Tokyo-Stromlo Photometry Survey (Matsuoka et al. 2008).

We carried out the follow-up photometry of a few dozen 1 $\mu$m excess sources, including the present three objects, before the final spectroscopy. The optical imaging observations were carried out during 2009 August–September, with a special $i$-band filter with the blueward transmission extending to 6300 Å (at the half of the maximum transmission) installed to the Imager mounted on the Australian National University (ANU) 2.3-m Advanced Technology Telescope at the Siding Spring Observatory. At the near-IR wavelengths, the SIRIUS camera (Nagashima et al. 1999; Nagayama et al. 2003) of the Infrared Survey Facility (IRSF) 1.4 m telescope at Sutherland, South African Astronomical Observatory was used for the follow-up observations. They were conducted in the two periods, 2009 June–July and September–October. The magnitudes listed in Table 1 are found to be robust in these follow-up photometry. The 1.8 m Microlensing Observations in Astrophysics (MOA; Bond et al. 2001; Sumi et al. 2003) II telescope is also used for our project, although the present three targets are not covered by the MOA observations.

### 2.2. *Spectroscopy*

Based on the revised photometry, we selected 15 objects with the strongest 1-$\mu$m excesses and obtained their spectra. The three T dwarfs found in the above targets are the subject of this paper, while the rest of them appear to be other classes of objects. The results of the whole observations will be presented in a next paper. The spectroscopy was carried out using the Gemini Multi-Object Spectrographs (GMOS; Hook et al. 2004) mounted on the Gemini North telescope (Program ID: GN-2010B-Q-102). The observation journal is given in Table 2. The R400-G5305 grating with the central wavelength set to 8500 Å was used with the blocking filter RG610-G0307, so that the wavelength range from 6500 Å to 10500 Å was covered. Since the targets are too faint to view on the acquisition images, we adopt either of the following acquisition techniques. For ULAS J0226+0051, the "blind offset" acquisition was performed using a nearby bright star as a reference source. For the other two targets without suitable nearby stars, we acquired the bright stars within a few arcminutes at the slit center and configured the instrument position angles so that the targets fall off-center of the slit. In order to avoid a large flux loss due to misalignment of the slit, which may be caused by the blind acquisitions, we adopted the relatively wide slit of $1''.5$ in width. It results in the moderate wavelength resolution of $R\sim600$, which is still enough for identifying the objects. The single exposure time was 900 s for all the science targets. The targets were offset by $10''$ along the spatial axis of the slit between the exposures, which enables good subtraction of the sky background with the prominent fringe patterns at the red part of the spectra.

The data were reduced in a standard manner using the Gemini IRAF[9] package, version 1.10. First the bias subtraction and flat fielding were performed, then the CuAr spectra were used to rectify and give the wavelength solutions to the images. The fringe patterns were successfully eliminated by subtracting the adjacent exposures.

[7] Funding for the SDSS and SDSS-II has been provided by the Alfred P. Sloan Foundation, the Participating Institutions, the National Science Foundation, the U.S. Department of Energy, the National Aeronautics and Space Administration, the Japanese Monbukagakusho, the Max Planck Society, and the Higher Education Funding Council for England. The SDSS Web site is http://www.sdss.org/. The SDSS is managed by the Astrophysical Research Consortium for the Participating Institutions. The Participating Institutions are the American Museum of Natural History, Astrophysical Institute Potsdam, University of Basel, University of Cambridge, Case Western Reserve University, University of Chicago, Drexel University, Fermilab, the Institute for Advanced Study, the Japan Participation Group, Johns Hopkins University, the Joint Institute for Nuclear Astrophysics, the Kavli Institute for Particle Astrophysics and Cosmology, the Korean Scientist Group, the Chinese Academy of Sciences (LAMOST), Los Alamos National Laboratory, the Max-Planck-Institute for Astronomy (MPIA), the Max-Planck-Institute for Astrophysics (MPA), New Mexico State University, Ohio State University, University of Pittsburgh, University of Portsmouth, Princeton University, the United States Naval Observatory, and the University of Washington.

[8] The UKIDSS magnitudes are taken from the Data Release (DR) 3 for consistency with the target selection strategy based on the DR3. While the updated magnitudes are now available, they are not significantly different from the values presented here.

[9] IRAF is distributed by the National Optical Astronomy Observatory, which is operated by the Association of Universities for Research in Astronomy, Inc., under cooperative agreement with the National Science Foundation.

TABLE 1
Red-optical and Near-IR Magnitudes

| Object | $i_{\rm AB}$ (mag) | $z_{\rm AB}$ (mag) | $Y_{\rm Vega}$ (mag) | $J_{\rm Vega}$ (mag) | $H_{\rm Vega}$ (mag) | $K_{\rm Vega}$ (mag) |
|---|---|---|---|---|---|---|
| ULAS J0128−0041 | >25.64 | 20.57 (0.04) | 18.48 (0.07) | 17.62 (0.05) | 16.91 (0.04) | 16.52 (0.06) |
| ULAS J0226+0051[a] | >25.88 | 21.32 (0.08) | 19.16 (0.11) | 18.33 (0.08) | 17.83 (0.12) | 17.69 (0.16) |
| ULAS J0321+0051 | >25.84 | 22.23 (0.17) | 20.06 (0.18) | 19.19 (0.10) | 18.76 (0.20) | 18.74 (0.26) |

Note. — Given above are the PSF magnitudes for the SDSS $i$ and $z$ bands and the $2''.8$ aperture magnitudes for the UKIDSS $Y$, $J$, $H$, and $K$ bands. Values in the parentheses represent $1\sigma$ errors, while $2\sigma$ upper limits are given for the non-detected sources. The magnitudes are extracted from the SDSS DR 7 and the UKIDSS DR 3.
[a]This object is identical to IfA 0230-Z1 ($J = 18.17 \pm 0.03$ mag and $H = 17.83 \pm 0.04$ in the MKO system) discovered by Liu et al. (2002).

TABLE 2
Observation Journal of Gemini/GMOS Spectroscopy

| Object | Date | Exp. Time (s) | Type |
|---|---|---|---|
| ULAS J0128−0041 | 2010 Aug. 30 | 1800 | Science target |
| ULAS J0226+0051 | 2010 Sep. 19 | 3600 | Science target |
| EG 131 | 2010 Sep. 20 | 120 | Standard star |
| ULAS J0321+0051 | 2010 Sep. 22 | 10800 | Science target |

Then the residual sky background was estimated from the fluxes of the nearby pixels in the spatial direction and removed. The instrument sensitivity was calibrated with the observed spectrum of the spectroscopic standard star EG 131. We did not observe a telluric standard star on each night, hence the accurate correction for the atmospheric absorption is not possible.

We show the reduced spectra in Figure 1. They are not detected above $3\sigma$ significance at the wavelengths $\lambda < 8000$ Å, where we give the broad-band $2\sigma$ upper limits calculated in the wavelength intervals $\lambda = 6500$–6800, 6800–7100, 7100–7400, 7400–7700, and 7700–8000 Å. Note that the $H_2O$ absorption bands at $\lambda \sim 9300$ Å are contaminated with the telluric absorptions.

## 3. ANALYSIS

### 3.1. *Spectral Type*

Since the signal-to-noise ratios of our spectra are not very high, we determine the spectral types of the targets with their broadband spectral energy distributions (SEDs) rather than with the individual absorption features. The extremely-red SEDs suggest that they are the members of brown dwarfs with the spectral types later than L. In Figure 1 we compare the observed spectra with those of the L8, T2, T5, and T8 dwarfs which are commonly used as the reference objects (anchor points) for the classification at the red optical wavelengths (Kirkpatrick et al. 1999; Burgasser et al. 2003), namely, 2MASSW J1632291+190441 (L8), SDSSp J125453.90−012247.4 (T2), 2MASSI J0559191−140448 (T5), and 2MASSI J0415195−093506 (T8). The three targets are clearly redder than the L8 dwarf and show the overall agreements with the T-dwarf spectra, while the spectral slopes at the longest wavelengths (> 9800 Å) indicate that they are not in late-T subclasses.

The classification of them as early-T type is also supported by their optical to near-IR colors. We show the $z - J$ versus $J - K$ two-color diagram of stars and brown dwarfs in Figure 2. The colors of O–M stars and L, T dwarfs are obtained from the compilation by Hewett et al. (2006), while the empirical mean relation between the colors of M–T dwarfs is taken from Kakazu et al. (2010). Note that all the near-IR magnitudes are consistently based on the Mauna Kea Observatories (MKO) system (Tokunaga et al. 2002), which is important because different photometric systems can lead to the different near-IR magnitudes by up to 0.4 mag for T dwarfs (Stephens & Leggett 2004). The three targets are located in the region occupied by the early-T dwarfs, and the most plausible classification would be T1 for ULAS J0128−0041, T2 for ULAS J0226+0051, and T3 for ULAS J0321+0051 (summarized in Table 3). However, we emphasize that the above typing is not meant to be conclusive: the uncertainty of ±1 subclass seems plausible. We note that ULAS J0321+0051 is one of the faintest T dwarfs known.

While ULAS J0128−0041 and ULAS J0321+0051 are the newly discovered T dwarfs, ULAS J0226+0051 has previously been reported by Liu et al. (2002). The object, named IfA 0230−Z1 in the discovery paper, was identified in the Institute for Astronomy (IfA) Deep Survey conducted at the University of Hawai'i. Liu et al. (2002) present a $H$-band spectrum as well as $I$, $z$, $J$, and $H$-band magnitudes of the object, from which they estimate a spectral type of T3–T4. Later the updated near-IR classification of T3 is given by Burgasser et al. (2006). Our spectral typing is consistent with these near-IR classifications considering the typical uncertainty of one spectral subclass.

### 3.2. *Distance, Proper Motion, and Variability*

We estimate the distances to the three T dwarfs by using the luminosity–spectral type relation provided by Liu et al. (2006). The $H$-band magnitudes are used for this purpose, since $H$-band luminosity of early-T dwarfs is relatively independent of the spectral subclasses which are not precisely known in the present case. Assuming the $H$-band absolute magnitude of $13.5 \pm 0.5$ mag (Liu et al. 2006) for T1–3 spectral types, the distance estimates to ULAS J0128−0041, ULAS J0226+0051, and ULAS J0321+0051 are $50 \pm 10$ pc, $70 \pm 20$ pc, and $110 \pm 30$ pc, respectively. The lower limit of the estimate for ULAS J0226+0051 is consistent with $49 \pm 9$ pc presented by Liu et al. (2002). As compiled by Kakazu et al. (2010), there are only a handful of spectroscopically con-

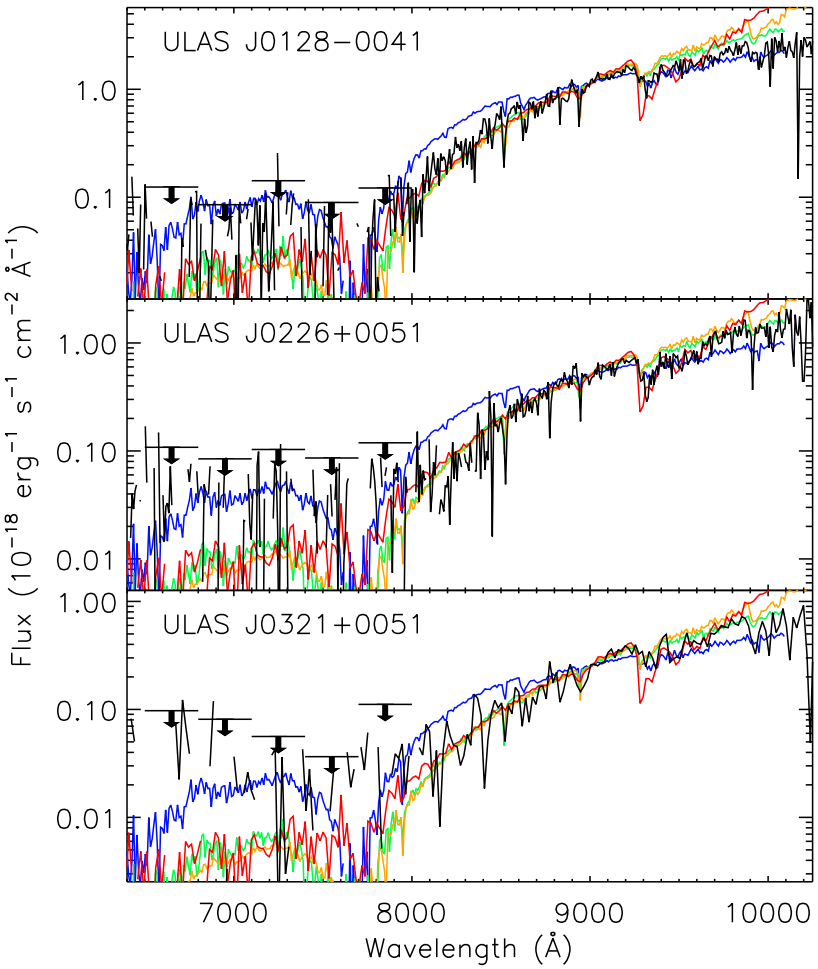


FIG. 1.— Gemini/GMOS spectra of the three T dwarfs (black). The horizontal lines with the arrows at $\lambda < 8000$ Å represent the broadband $2\sigma$ upper limits of the observed fluxes. The template spectra of the L8 (blue), T2 (green), T5 (orange), and T8 (red) dwarfs, normalized at $\lambda = 9000$ Å, are also plotted for comparison.

TABLE 3
ESTIMATED PROPERTIES

| Object | Spectral Type | Distance (pc) | Proper Motion (mas yr$^{-1}$) | Transverse Velocity (km s$^{-1}$) |
|---|---|---|---|---|
| ULAS J0128−0041 | Early-T (T1) | 50 ± 10 | 150 ± 30 | 40 ± 10 |
| ULAS J0226+0051 | Early-T (T2) | 70 ± 20 | 290 ± 140 | 100 ± 50 |
| ULAS J0321+0051 | Early-T (T3) | 110 ± 30 | ··· | ··· |

NOTE. — Spectral subclasses given in the parenthesis are not conclusive. See the text.

firmed T dwarfs known today at distances beyond 60 pc, and only a few beyond 100 pc. Therefore the objects presented here are among the most distant T dwarfs.

The three dwarfs are found in the SDSS southern equatorial stripe, where the intensive repeat scans were carried out in the SDSS-II Supernova Survey. The dense temporal coverage over several years allows us a simple time-series analysis of the objects. We retrieve all the $z$-band images of the target fields from the SDSS DR 7 archive (Abazajian et al. 2009) and create the stacked images of each year. The stacking is not performed when less than five images are available in a year. It results in the deep images of the years 2002, 2005, 2006, 2007 for ULAS J0128−0041, years 2002, 2003, 2005, 2006, 2007 for ULAS J0226+0051, and years 2002, 2005, 2006, 2007 for ULAS J0321+0051. We measure the coordinates and magnitudes of the objects with the *Source Extractor*, version 2.5 (Bertin & Arnouts 1996), if the targets are detected on the stacked images (more than four adjacent pixels above $1.5\sigma$ of the local background are defined as detections). The results for the detected sources are summarized in Table 4. Unfortunately, ULAS J0321+0051 is too faint to be detected on any of the year-based stacked images. The coordinates are shown as the relative offsets (milliarcsecond; mas) from the UKIDSS positions. The magnitudes are measured in $3''.0$ apertures and are corrected so that the mean measured magnitudes match the point-spread function (PSF) magnitudes listed in Table 1, whose differences represent the mean aperture losses ($-0.25$ and $-0.20$ mag are added to the measured magnitudes of ULAS J0128−0041 and ULAS J0226+0051, respectively).

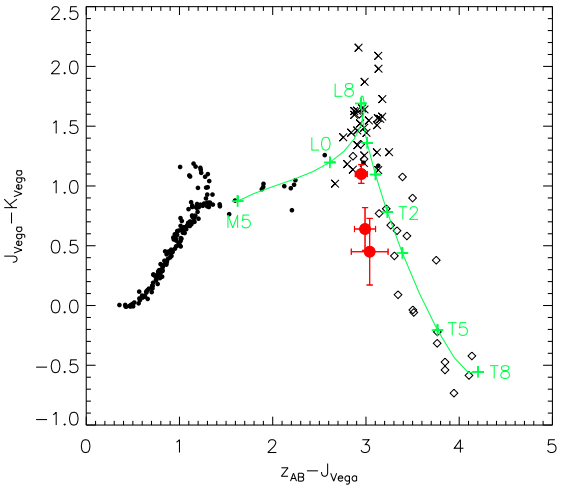


FIG. 2.— $z - J$ vs. $J - K$ two-color diagram of stars and brown dwarfs. The small circles represent O–M stars while the crosses and the diamonds represent L and T dwarfs, respectively, taken from Hewett et al. (2006). The empirical mean relation between the colors of M5–T8 dwarfs (Kakazu et al. 2010) are also plotted (green line) with the plus marks placed at the positions of M5, L0, L8, T0, T1, T2, T3, T5, and T8. Our targets are shown by the red circles with error bars (ULAS J0128−0041, ULAS J0226+0051, and ULAS J0321+0051, from top to bottom).

The positional information of ULAS J0226+0051 is also available from Liu et al. (2002), who report the coordinate obtained on the epoch of 2001 October with the Suprime-Cam mounted on the Subaru telescope. Its relative offset from the UKIDSS position is ΔR.A. = +0–+1300 mas and Δdecl. = +300 mas (since Liu et al. (2002) round the R.A. to first decimal place in the paper, we assume it to be $02^h26^m37^s.55$–$37^s.64$). The derived Δdecl. value, on the year 2001, is clearly inconsistent with the increasing declination of this object indicated in Table 4. The major reason for this inconsistency (though within an arcsecond) is likely the different astrometric calibrations adopted, therefore we do not use the Suprime-Cam coordinate in the following arguments.

Considering the typical SDSS astrometric uncertainty of 100 mas at the limiting depth (Pier et al. 2003), significant spatial movements are detected for the two dwarfs in Table 4. We derive the proper motions from the two measurements with the longest baselines, i.e., 2002–2007 for ULAS J0128−0041 and 2006–2007 for ULAS J0226+0051. The transverse velocities are then calculated using the distances estimated above. We list the results in Table 3. These kinematic properties provide vital information not only on the structure of the Galaxy but also on the ages of the substellar systems when combined with the appropriate models. The derived transverse velocity of ULAS J0128−0041 is in agreement with the median value ∼ 30 km $s^{-1}$ of early-T dwarfs found by Faherty et al. (2009), suggesting that the object is a member of typical field T dwarfs. On the other hand, ULAS J0226+0051 may have higher velocity than the typical objects, suggesting that this dwarf may be an older member of the Galactic thick disk or halo population (e.g., Nordström et al. 2004).

As for the source brightness, we find no detectable long-term variations in the $z$ band. The Suprime-Cam $z$-band photometry gives $z_{AB} = 21.44 \pm 0.15$ mag for ULAS J0226+0051 (Liu et al. 2002) when the Vega-to-AB magnitude conversion of +0.533 mag (Hewett et al. 2006) is used, which is also in agreement with those listed in Table 4. Note that the Suprime-Cam $z$-band filter is very similar to that of the SDSS. There have been several observational searches for short-term (minutes to weeks) variability in brown dwarfs at the L/T transition (e.g., Enoch et al. 2003; Clarke et al. 2008; Artigau et al. 2009), which could give a stringent constraint on the models of their atmospheres. Here our inquiry into the long-term (years) variations is not based on a model prediction, but rather motivated by a need for the *empirical* constraints on the stability of brown-dwarf colors, which are essential in defining the selection strategies of high-redshift quasars or brown dwarfs from photometry data obtained on different dates (see Section 2.1). The lack of significant variations over a few times 0.1 mag may indicate that the variability of early-T dwarfs do not cause significant uncertainty in the selection strategies, although more samples, including other subclasses of brown dwarfs and time-series near-IR data, are needed for a firm conclusion.

TABLE 4
TIME-SERIES ANALYSIS

| Object | Year | ΔR.A. (mas) | Δdecl. (mas) | $z_{AB}$ (mag) |
|---|---|---|---|---|
| ULAS J0128−0041 | 2002 | +320 | +170 | 20.57 (0.15) |
| | 2005 | +20 | −40 | 20.55 (0.09) |
| | 2006 | −60 | −30 | 20.59 (0.09) |
| | 2007 | −350 | −210 | 20.55 (0.08) |
| ULAS J0226+0051 | 2006 | +190 | −200 | 21.32 (0.14) |
| | 2007 | +350 | +40 | 21.32 (0.15) |

NOTE. — Coordinates are given as the relative offsets from the UKIDSS positions. Values in the parenthesis represent 1$\sigma$ photometry errors.

## 4. SUMMARY

This is the first paper from our follow-up observation program of 1 $\mu$m excess sources in the UKIDSS. In this paper we present the newly discovered two brown dwarfs, ULAS J0128−0041 and ULAS J0321+0051, as well as the re-discovered ULAS J0226+0051 (IfA 0230-Z1), in the SDSS southern equatorial stripe. The follow-up imaging observations were carried out with the optical Imager on the ANU 2.3-m telescope and the near-IR SIRIUS camera on the IRSF telescope. Then we obtained their red optical (6500–10500 Å) spectra with the GMOS on the Gemini North telescope in order to identify the targets. The spectra reveal that the objects belong to early-T dwarf subclasses, which is also supported by their optical to near-IR colors. ULAS J0321+0051 turns out to be one of the faintest currently-known T dwarfs.

We estimate the distances to the dwarfs to be 50–110 pc from the empirical luminosity–spectral type relation of brown dwarfs. By taking advantage of the dense temporal coverage of the target fields achieved by the SDSS-II Supernova Survey, we create the stacked images of each year during 2002–2007 and conduct a simple time-series analysis. As a result, we find the significant proper motions of 150 and 290 mas $yr^{-1}$, which are converted to the transverse velocities of 40 and 100 km $s^{-1}$, for ULAS J0128−0041 and ULAS J0226+0051, respectively. It suggests that ULAS J0128−0041 is a member of typical field T dwarfs, while ULAS J0226+0051 may have the

higher velocity than average and be an older member of the Galactic thick disk or halo population. We also look into the possible long-term (a-few-year) brightness variations of the two objects, and find no detectable variations above a few times 0.1 mag. This suggests that the variability of early-T dwarfs does not cause significant uncertainty in the selection strategies of high-redshift quasars or brown dwarfs with photometry data taken on different dates, although more observations are needed to reach a firm conclusion.

We are grateful to the referee, Sandy Leggett, for giving very useful comments and suggestions. We thank the staff of the Siding Spring Observatory, the South African Astronomical Observatory, and the Gemini Observatory (including Alexander Fritz) for the support during the observations. The IRSF team at Nagoya University, Kyoto University, and the National Astronomical Observatory of Japan has provided a great help for the IRSF observations. This work was supported by Grants-in-Aid for Scientific Research (21840027, 22684005) and the Global COE Program of Nagoya University "Quest for Fundamental Principles in the Universe" from JSPS and MEXT of Japan.

REFERENCES

Abazajian, K. N., et al. 2009, ApJS, 182, 543
Artigau, É., Bouchard, S., Doyon, R., & Lafrenière, D. 2009, ApJ, 701, 1534
Becklin, E. E., & Zuckerman, B. 1988, Nature, 336, 656
Bertin, E., & Arnouts, S. 1996, A&AS, 117, 393
Bond, I. A., et al. 2001, MNRAS, 327, 868
Burgasser, A. J., Geballe, T. R., Leggett, S. K., Kirkpatrick, J. D., & Golimowski, D. A. 2006, ApJ, 637, 1067
Burgasser, A. J., Reid, I. N., Leggett, S. K., Kirkpatrick, J. D., Liebert, J., & Burrows, A. 2005, ApJ, 634, L177
Burgasser, A. J., Kirkpatrick, J. D., Liebert, J., & Burrows, A. 2003, ApJ, 594, 510
Clarke, F. J., Hodgkin, S. T., Oppenheimer, B. R., Robertson, J., & Haubois, X. 2008, MNRAS, 386, 2009
Dahn, C. C., et al. 2002, AJ, 124, 1170
Delorme, P., et al. 2008, A&A, 484, 469
Enoch, M. L., Brown, M. E., & Burgasser, A. J. 2003, AJ, 126, 1006
Epchtein, N., et al. 1999, A&A, 349, 236
Faherty, J. K., Burgasser, A. J., Cruz, K. L., Shara, M. M., Walter, F. M., & Gelino, C. R. 2009, AJ, 137, 1
Fan, X., et al. 2006, AJ, 131, 1203
Frieman, J. A., et al. 2008, AJ, 135, 338
Hewett, P. C., Warren, S. J., Leggett, S. K., & Hodgkin, S. T. 2006, MNRAS, 367, 454
Hook, I. M., Jørgensen, I., Allington-Smith, J. R., Davies, R. L., Metcalfe, N., Murowinski, R. G., & Crampton, D. 2004, PASP, 116, 425
Kakazu, Y., Hu, E. M., Liu, M. C., Wang, W.-H., Wainscoat, R. J., & Capak, P. L. 2010, ApJ, 723, 184
Kirkpatrick, J. D. 2005, ARA&A, 43, 195
Kirkpatrick, J. D., et al. 1999, ApJ, 519, 802
Knapp, G. R., et al. 2004, AJ, 127, 3553
Lawrence, A., et al. 2007, MNRAS, 379, 1599
Liu, M. C., Leggett, S. K., Golimowski, D. A., Chiu, K., Fan, X., Geballe, T. R., Schneider, D. P., & Brinkmann, J. 2006, ApJ, 647, 1393
Liu, M. C., Wainscoat, R., Martín, E. L., Barris, B., & Tonry, J. 2002, ApJ, 568, L107
Matsuoka, Y., et al. 2008, ApJ, 685, 767
Nagashima, C., et al. 1999, Star Formation 1999, 397
Nagayama, T., et al. 2003, Proc. SPIE, 4841, 459
Nakajima, T., Oppenheimer, B. R., Kulkarni, S. R., Golimowski, D. A., Matthews, K., & Durrance, S. T. 1995, Nature, 378, 463
Nordström, B., et al. 2004, A&A, 418, 989
Pier, J. R., Munn, J. A., Hindsley, R. B., Hennessy, G. S., Kent, S. M., Lupton, R. H., & Ivezić, Ž. 2003, AJ, 125, 1559
Skrutskie, M. F., et al. 2006, AJ, 131, 1163
Stephens, D. C., & Leggett, S. K. 2004, PASP, 116, 9
Sumi, T., et al. 2003, ApJ, 591, 204
Tokunaga, A. T., Simons, D. A., & Vacca, W. D. 2002, PASP, 114, 180
Venemans, B. P., McMahon, R. G., Warren, S. J., Gonzalez-Solares, E. A., Hewett, P. C., Mortlock, D. J., Dye, S., & Sharp, R. G. 2007, MNRAS, 376, L76
Vrba, F. J., et al. 2004, AJ, 127, 2948
Warren, S. J., et al. 2007, MNRAS, 375, 213
Willott, C. J., et al. 2010, AJ, 139, 906
York, D. G., et al. 2000, AJ, 120, 1579